Characterization of collagen fibers by means of texture analysis of second harmonic generation images using orientation-dependent gray level co-occurrence matrix method

Wenyan Hu
Hui Li
Chunyou Wang
Shanmiao Gou
Ling Fu

Characterization of collagen fibers by means of texture analysis of second harmonic generation images using orientation-dependent gray level co-occurrence matrix method

Wenyan Hu,a,b,* Hui Li,a,b,* Chunyou Wang,c Shanmiao Gou,c and Ling Fua,b
aWuhan National Laboratory for Optoelectronics-Huazhong University of Science and Technology, Britton Chance Center for Biomedical Photonics, Wuhan 430074, China
bHuazhong University of Science and Technology, Key Laboratory of Biomedical Photonics of Ministry of Education, Wuhan 430074, China
cHuazhong University of Science and Technology, Pancreatic Surgery Center in Union Hospital, Wuhan 430074, China

Abstract. Collagen is the most prominent protein in the human body, making up 30% of the total protein content. Quantitative studies have shown structural differences between collagen fibers of the normal and diseased tissues, due to the remodeling of the extracellular matrix during the pathological process. The dominant orientation, which is an important characteristic of collagen fibers, has not been taken into consideration for quantitative collagen analysis. Based on the conventional gray level co-occurrence matrix (GLCM) method, the authors proposed the orientation-dependent GLCM (OD-GLCM) method by estimating the dominant orientation of collagen fibers. The authors validated the utility of the OD-GLCM method on second harmonic generation (SHG) microscopic images of tendons from rats with different ages. Compared with conventional GLCM method, the authors' method has not only improved the discrimination between different tissues but also provided additional texture information of the orderliness of collagen fibers and the fiber size. The OD-GLCM method was further applied to the differentiation of the preliminary SHG images of normal and cancerous human pancreatic tissues. The combination of SHG microscopy and the OD-GLCM method might be helpful for the evaluation of diseases marked with abnormal collagen morphology. © 2012 Society of Photo-Optical Instrumentation Engineers (SPIE). [DOI: 10.1117/1.JBO.17.2.026007]

Keywords: collagen fibers; dominant orientation; gray level co-occurrence matrix; orientation-dependent gray level co-occurrence matrix; second harmonic generation microscopy; texture analysis.

Paper 11446 received Aug. 17, 2011; revised manuscript received Nov. 24, 2011; accepted for publication Dec. 14, 2011; published online Feb. 23, 2012.

1 Introduction

As the chief structural protein of all vertebrates, collagen accounts for approximately 30% of body protein. More than 90% of the extracellular protein in the tendon and bone and more than 50% in the skin consist of collagen.[1] The characteristics of collagen reveal important information with regards to the health status.[2–4] Many studies have shown that the collagen fibers are irregularly disordered without well-defined orientation in pathological samples, while the morphology of the collagen fibers is highly structured in normal samples.[4–9] For instance, the biopsies from patients with epithelial ovarian cancer exhibited a loss of fine structure and structural organization with wavy, collagen bands, whereas the normal biopsies exhibited normotypic structured collagen fibrils near the epithelial surface.[4] Therefore, detailed characterization of the collagen morphology is important because structural modifications of the fibrillar matrix are associated with various physiologic processes such as aging, diabetes, wound healing, and cancer.[10]

Conventional approaches to characterize collagen include standard tissue staining, in situ hybridization, enzyme linked immunosorbent assays (ELISA), scanning and transmission electron microscopy, and polarization microscopy. Over the last decade, second harmonic generation (SHG) microscopy emerged as an *in vivo* imaging modality to provide high-resolution three-dimensional images of collagen fibers in thick specimens without the need for sample staining and processing.[1–3,11–17] Moreover, collagen has a highly crystalline triple-helix structure,[18] which is a chiral molecule. The non-centrosymmetrical structure of fibrillar collagen makes it the major source of the SHG signals in biological materials.[8,10,11,14,18,19] Recently, SHG imaging has been commonly applied in studies of diseases marked with collagen, such as melanomas,[16] epithelial ovarian cancer,[4] osteogenesis imperfecta[9] and so on.

In order to advance the accuracy and efficiency of future clinical diagnosis, the morphology of collagen fibers revealed by SHG imaging have been quantitatively described by texture analysis. Texture analysis approaches can be categorized into statistical, structural, model-based, and transform-based methods.[20,21] For medical applications, the statistical methods are extensively used, since they can achieve higher discrimination indexes.[21] As the most frequently cited statistical method,[20–22] the gray level co-occurrence matrix (GLCM) has been applied to a variety of fields for decades, including texture analysis of

---

*These authors contributed equally to this work. Their e-mails are wyuan-hu@gmail.com and huldali@126.com, respectively.

Address all correspondence to: Ling Fu, Wuhan National Laboratory for Optoelectronics-Huazhong University of Science and Technology, Britton Chance Center for Biomedical Photonics, Wuhan 430074, China. Tel: (86) 27-87792033; Fax: (86) 27- 87792034; E-mail: lfu@mail.hust.edu.cn

remote sensing images,[13,23–25] surface roughness analysis,[26] the extraction of significant patterns from industrial flotation froths,[27] and quantitative analysis of medical images.[21,28–34]

Combined with SHG imaging, the GLCM approach has been used to quantitatively analyze the collagen fibers.[4,35] But it simply classifies different biological tissues by the feature values without providing any information directly associated with the geometrical arrangement of collagen fibrillar bundles. Generally, GLCM features along one or two of the four specific directions of 0 deg, 45 deg, 90 deg, and 135 deg or average feature values along these four directions are extracted to quantitatively analyze the SHG images.[4,29,31,32,36] However, the dominant orientation of the collagen fibers is usually ignored in the conventional GLCM analysis. Since the orientation is an important characteristic of collagen fibers with a filamentous structure, the GLCM features calculated along the dominant orientation of collagen fibers are different from those calculated along the other directions. As a result, the texture information obtained from the feature curves is dependent on the direction selected in GLCM analysis. By combining the dominant orientation of collagen fibers into the GLCM analysis, the GLCM feature curves calculated may provide more information for detailed morphological characterization of the collagen fibers, thus leading to further sights into various physiological and pathological processes, such as the structural modification of the extracellular matrix during the migration and invasion of tumor cells.

In order to take into account the dominant orientation of collagen fibers and extract more comprehensive morphological information, we proposed the orientation-dependent GLCM (OD-GLCM) method based on the dominant orientation of collagen fibers. The OD-GLCM method was compared with the conventional GLCM method by quantitative analysis of SHG images of rat tendons. It was further applied to the differentiation of SHG images from normal and cancerous human pancreatic tissues at different stages.

2 Materials and Methods

2.1 Preparation of the Artificial Images and the Biological Samples

To validate the dependence of GLCM analysis of collagen fibers on the direction selected, we have created model images, which consist of strips with regular and random structure [Figs. 1(a), 1(c), 1(e), and 1(g)] similar to the most representative patterns of collagen fibers.[4,37–39] The white strips were manually created by Visio (Microsoft) and converted to gray-level synthetic images with 512×512 pixels by adding Gaussian white noise of mean 0 and variance 0.1 to the black and white images using MATLAB (The MathWorks) function "imnoise." The width of the strips are manually set to be 13 pixels [Figs. 1(a), 1(c), and 1(g)] and 20 pixels [Fig. 1(e)] for different model images, respectively. Besides, the strips in the relatively regular images [Figs. 1(a), 1(c), and 1(e)] were set to be aligned along the direction of 145 deg, 50 deg, and 50 deg, respectively.

The *ex vivo* rat tendons, which can be divided into the old ($n = 6$) and young ($n = 6$) groups, were sandwiched between the microscope slide and cover glass in phosphate buffered saline and imaged within 1 h after dissection. The old group included three seven-week-old rats, two 10-week-old rats, and one eight-month-old rat, and the young group included six 10-day-old rats. Seven human pancreatic specimens, including one normal pancreatic tissue beside the tumor, and four well
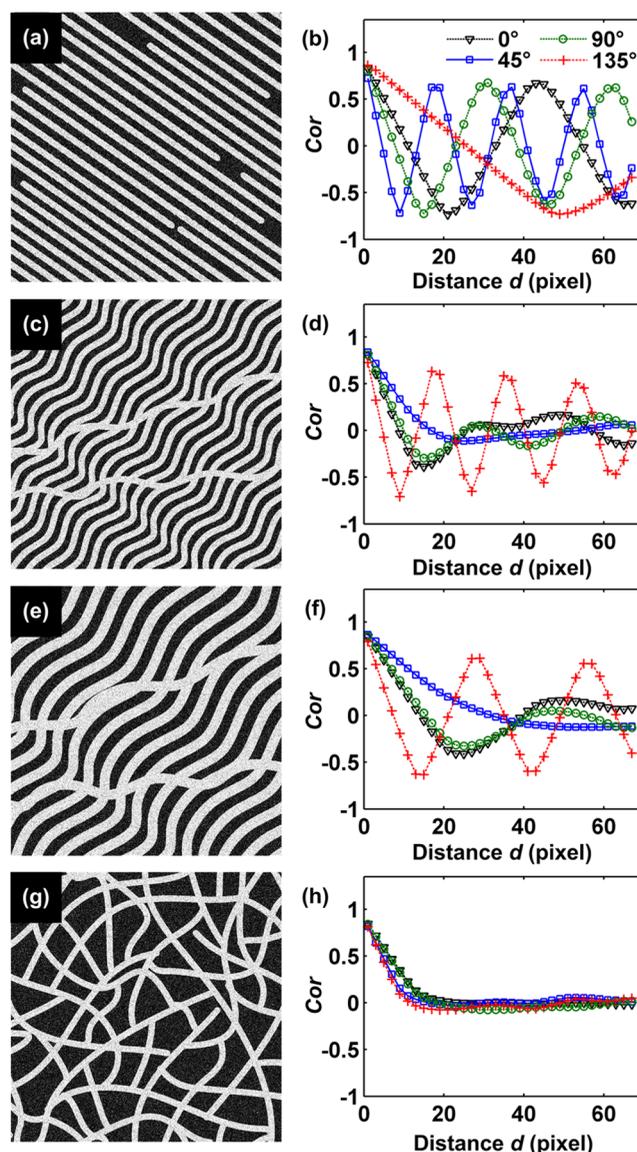
Fig. 1 GLCM analysis was performed for [(a), (c), (e) and (g)] the model images consisting of strips arranged in regular and random structure. The second column shows [(b), (d), (f) and (h)] Cor curves as a function of d in the directions of 0 deg, 45 deg, 90 deg, and 135 deg corresponding to the images in the first column. Note: GLCM = gray level co-occurrence matrix.

differentiated, one poor differentiated, as well as one liver metastasized pancreatic cancer tissues, were collected during a surgical resection from pancreatic cancer patients, respectively. All the patients who participated in the study were provided written informed consent and ethical approval for the study was obtained from the institutional review board. The specimens were immersed in phosphate buffered saline and kept in ice before multiphoton microscopic imaging. They were imaged in the same way as the rat tendons within 3 h.

2.2 SHG Microscope System

For SHG imaging, a Ti:Sapphire laser (Spectra-Physics, Mai Tai) with a repetition rate of 80 MHz was used as the excitation source. The 750-nm output of the laser system was delivered to a modified commercial microscope (Fluoview 1000, Olympus)

Hu et al.: Characterization of collagen fibers by means of texture analysis...

and focused onto the sample through an objective ($60 \times /1.2$ NA water-immersion, Olympus). The backscattered SHG signal was collected by the same objective and filtered by a band-pass filter (330 to 385 nm) before the detection of the photomultiplier tube. The scanning rate is 4 to 10 μs/pixel and the average excitation power on the surface of the sample is about 8 to 15 mW. The SHG signal was confirmed by the property of wavelength dependence, since there was no signal detected in the 330 to 385 nm range at longer excitation wavelength such as 780 nm, while the fluorescence signal from the fibers could still be detected in the 515 to 560 nm range.

2.3 Image Pre-Processing

The SHG images were pre-processed using the MATLAB (The MathWorks) function "imadjust" for gray level adjustment to increase the contrast of the image, so that the intensities of the SHG signal acquired for different samples are comparable. Particularly, in order to improve the signal-to-noise ratio of SHG imaging from pancreatic samples, up to four consecutive optical slices were averaged, and the adaptive threshold algorithm with a kernel size of 51×51 pixels[3] was used before the gray level adjustment, since the estimated fiber size can be affected by the noise level without pre-processing.

2.4 Dependence of GLCM Analysis on the Direction Selected

For an image with g gray levels, the GLCM is an estimate of the second-order joint probability $p(i,j|d,g,\theta)$ of any two pixels with gray level i and j ($0 \leq i < g$, $0 \leq j < g$), which apart from each other with d pixel distance along direction θ.[20,36] In this paper, the most commonly used GLCM feature calculated from $p(i,j|d,g,\theta)$ named correlation (Cor) is discussed. The equation of Cor is given as below:[36,40]

$$\text{Cor} = \sum_{i,j} \frac{(i - \mu_i)(j - \mu_j)p(i,j)}{\sigma_i \sigma_j}, \quad (1)$$

where

$$\mu_i = \sum_{i,j} i \cdot p(i,j), \quad (2)$$

$$\mu_j = \sum_{i,j} j \cdot p(i,j), \quad (3)$$

$$\sigma_i = \sqrt{\sum_{i,j} (i - \mu_i)^2 p(i,j)}, \quad (4)$$

$$\sigma_j = \sqrt{\sum_{i,j} (j - \mu_j)^2 p(i,j)}. \quad (5)$$

All the Cor curves along the four specific directions of 0 deg, 45 deg, 90 deg, and 135 deg were calculated for the model images. One of the four directions proximal to the texture dominant orientation is defined as θ^* in Eq. (6). For model images with orientation to a certain extent [Figs. 1(a), 1(c), and 1(e)], the Cor curves calculated along the direction of θ^* are different from those calculated along the other

directions [Figs. 1(b), 1(d), and 1(f)]. It suggests that the GLCM analysis for collagen fibers is dependent on the direction selected to calculate the GLCM features. In order to take the dominant orientation of collagen fibers into consideration, we proposed the OD-GLCM method to get more comprehensive information for quantitative morphological analysis of collagen fibers.

$$\theta^* = \arg \max_{\theta \in X} \text{Cor}(\theta), \quad X = (0, 45, 90, 135 \text{ deg}). \quad (6)$$

2.5 Dominant Orientation of Collagen Fibers

To estimate the dominant orientation of collagen fibers, the direction in GLCM calculation was divided into four parts, including (0 deg $\pm$22 deg), (45 deg $\pm$22 deg), [90 deg $\pm$22 deg), (135 deg $\pm$22 deg). We calculated the Cor along all the directions θ in the range of $\theta^* - 22$ deg to $\theta^* + 22$ deg [Fig. 2(a)] by rotating the image by θ clockwise and then cropping the image to square dimension using MATLAB (The MathWorks). It was found that the largest value corresponds to the dominant orientation of collagen fibers, which $\hat{\theta}$ is defined as in Eq. (7).

$$\hat{\theta} = \arg \max_{\theta \in X} \text{Cor}(\theta),$$
$$X = (x|\theta^* - 22 \text{ deg} \leq x \leq \theta^* + 22 \text{ deg}) \quad (7)$$

2.6 Estimation of the Orderliness of Collagen Fibers and the Fiber Size

As can be seen from the Cor curves as a function of θ for model images [Fig. 2(b)], the curve of the highly regular image shows an obvious peak at the dominant texture orientation while the curve of the random image is flat. Therefore, the standard deviation of Cor along all the directions in the range from $\theta^* - 22$ deg to $\theta^* + 22$ deg can be used to describe the orderliness of the texture, which is defined as σ_{Cor} in Eq. (8).

$$\sigma_{\text{Cor}} = \sqrt{\frac{1}{44} \sum_{\theta=\theta*-22°}^{\theta*+22°} [\text{Cor}(\theta) - \bar{\text{Cor}}(\theta)]^2}, \quad (8)$$

$$\text{where } \bar{\text{Cor}}(\theta) = \frac{1}{45} \sum_{\theta=\theta*-22°}^{\theta*+22°} \text{Cor}(\theta).$$
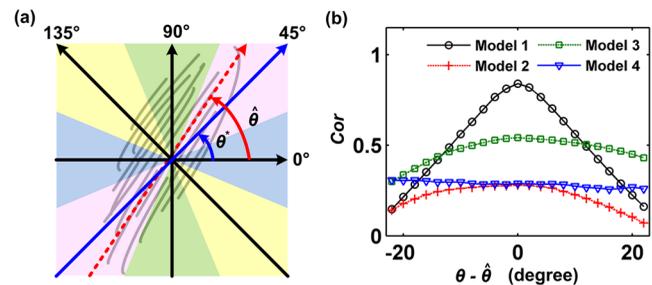
Fig. 2 (a) The direction used in GLCM calculation can be divided into four parts based on the four directions of 0 deg, 45 deg, 90 deg, and 135 deg. (b) The Cor along all the directions in the range from $\hat{\theta}-$22 deg to $\hat{\theta}+22$ deg. Note: GLCM = gray level co-occurrence matrix.

In addition, the Cor curves as a function of d for the model images with highly linear strips show periodic fluctuation [Figs. 1(b), 1(d), and 1(f)], which may provide information about the size of the strips. Based on the estimation of texture dominant orientation, the d value corresponding to the first valley of the Cor curves along the direction vertical to the dominant orientation was calculated and it was converted to length unit according to the size of the image to reflect the width of the collagen fibers.

3 Results

3.1 Analysis of Model Images

For the images with a relatively regular texture, the estimated dominant orientation was close to the true value (Table 1). The standard deviations of Cor (σ_{Cor}) for different model images were calculated (Table 1). It shows that the σ_{Cor} value increases as the texture of the image becomes more regular.

The Cor curve as a function of d along the direction vertical to the dominant orientation was used to reflect the size of the texture. As shown in Fig. 3(a) and Table 1, the d value corresponding to the first valley is close to the size of the strips in the model images [Figs. 1(a), 1(c), and 1(e)].

Compared with the conventional GLCM method, the patterns of the OD-GLCM Cor curves provide better discrimination between the regular and random images (Fig. 3). Besides, the orderliness can be estimated and the fluctuation of the OD-GLCM Cor curves for the images with a relatively regular texture shows quantitative relation with the fiber size (Table 1), allowing more detailed characterization of the texture morphology.

3.2 Analysis of Tendons from Rats with Different Ages

To demonstrate the effectiveness of the OD-GLCM method on biomedical samples, we applied it to SHG images of tendons and compared it with the conventional GLCM method. The SHG images of tendons from the old rat group [Fig. 4(a)] and the young rat group [Fig. 4(b)] were obtained by the SHG microscope system. Compared with the relatively random collagen fibers of tendons from the young rats, those of the old rats are orderly arranged with obvious orientation and uniform texture.

For the SHG images of the tendon samples, the Cor curves as a function of d are calculated by the OD-GLCM and the conventional GLCM method, respectively [Fig. 4(c)]. The Cor

Fig. 3 (a) The Cor curves calculated along the direction vertical to the dominant orientation from OD-GLCM show significantly different patterns between the regular and random model images, compared with (b) the average Cor curves of 0 deg, 45 deg, 90 deg, and 135 deg using conventional GLCM method. Model 1, Model 2, Model 3, and Model 4 represent the four model images (a), (c), (e), and (g) in Fig. 1, respectively. The estimated fiber size is indicated by the word size in red arrows. Note: OD-GLCM = orientation-dependent GLCM; GLCM = gray level co-occurrence matrix.

curves of the two groups of tendon samples calculated using the conventional GLCM method are relatively flat and close to each other. By contrast, the Cor curves calculated by the OD-GLCM method show significantly different patterns, allowing the discrimination of the collagen texture between the two groups of tendon samples.

The orderliness and size of the collagen fibers are further characterized using the OD-GLCM method. Compared with
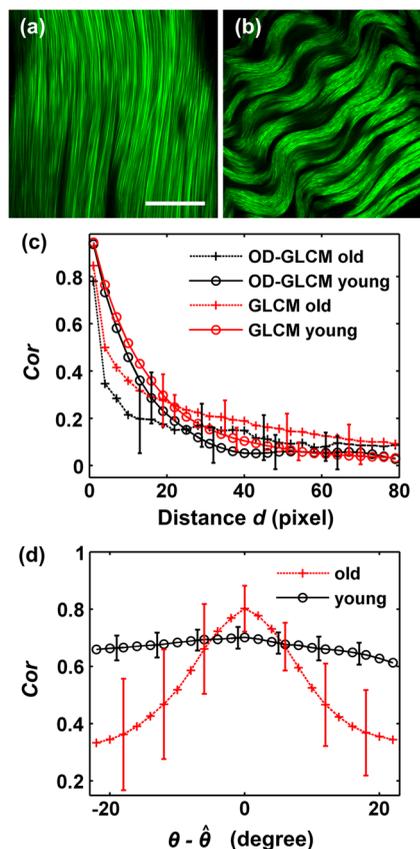
Fig. 4 Comparison of conventional average GLCM analysis method and the OD-GLCM method based on the SHG images of tendons from (a) six old rats and (b) six young rats. The Cor curves as a functin of (c) d and (d) θ are calculated respectively. *Bars*, SD. Scale bar = 30 μm. Note: GLCM = gray level co-occurrence matrix; OD-GLCM = orientation-dependent GLCM.

Table 1 The estimated dominant orientation, orderliness, and fiber size of model images.

	$\hat{\theta}$/ deg			Fiber size/pixel	
	Estimated	True	σ_{Cor}	Estimated	True
Model 1	145	145	0.31	12	13
Model 2	49	50	0.06	13	13
Model 3	45	50	0.06	20	20
Model 4	70	—	0.01	23	13

Table 2 The estimated orderliness and size of collagen fibers of the tendon samples from rats with different ages (mean ±SD). t test on log-transformed σ_{Cor} and fiber size was done, for σ_{Cor}, $P = 0.000007$; for fiber size, $P = 0.000003$; $n = 6$, old; $n = 6$, young.

	σ_{Cor}	Fiber size/μm
old	0.18 ± 0.05	2.9 ± 0.7
young	0.05 ± 0.01	8.9 ± 1.6

the tendon samples from the young rats, an obvious peak of the Cor curves as a function of θ can be observed for the SHG images of the old rats [Fig. 4(d)]. Besides, the quantitative descriptor σ_{Cor} for the tendon samples from the old rats show significantly higher values than those from the young rats (Table 2, $P = 0.000007$, $n = 6$, t test on log-transformed σ_{Cor}), indicating that the collagen fibers are more aligned than those of the young rats. In addition, the fiber size can be estimated based on the Cor curves calculated along the direction vetical to the dominant orientation (Table 2). The estimated values show that the collagen fibers of the tendons from the old rats are significantly thinner than those from the young rats ($P = 0.000003$, $n = 6$, t test on log-transformed fiber size). The above characteristics acquired by the OD-GLCM method are consistent with the qualitative appearances of collagen fibers in the SHG images [Figs. 4(a) and 4(b)].

3.3 Differentiation of Normal and Cancerous Human Pancreatic Tissues

We applied the OD-GLCM method in the differentiation of SHG images of normal and cancerous human pancreatic samples. The images were obtained by the SHG microscope system (Fig. 5).
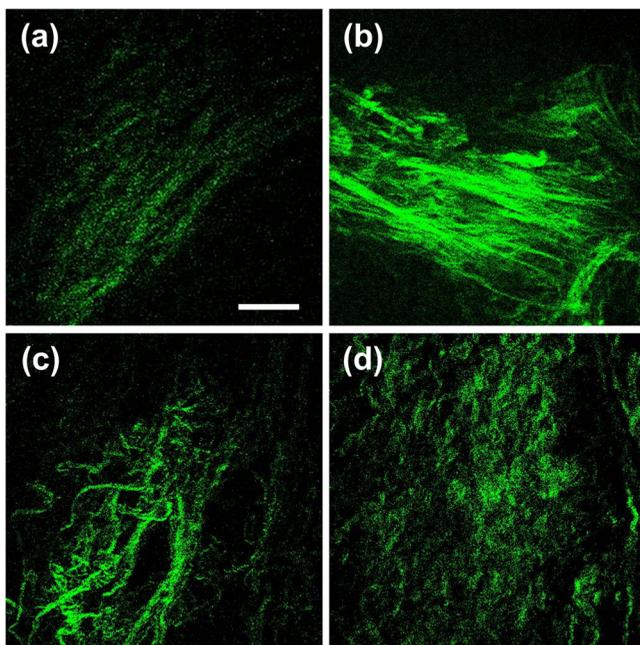
Fig. 5 SHG images of normal and cancerous human pancreatic samples. (a) normal pancreatic tissue; (b) well differentiated pancreatic cancer tissue; (c) poor differentiated pancreatic cancer tissue; (d) liver metastasis from pancreatic cancer. Scale bar = 40 μm.

Images of the normal and the well differentiated pancreatic cancer tissue [Figs. 5(a) and 5(b)] show a linear arrangement of collagen fibers. The tiny difference is that collagen fibers of the well differentiated pancreatic cancer tissue are slightly staggered and thinner than those of the normal tissues. In contrast, collagen fibers of the poor differentiated pancreatic cancer tissue are crimped and show a lack of regularity [Fig. 5(c)], while those of the liver metastasis from pancreatic cancer gather into massive clumps and completely lose the original linear pattern [Fig. 5(d)].

Comparison analysis of the pancreatic SHG images based on the OD-GLCM method is shown in Fig. 6. It can be observed that the normal and cancerous pancreatic tissues can be easily differentiated by the Cor curves calculated along the direction vertical to the dominant orientation of the collagen fibers [Fig. 6(a)]. The Cor curve of the normal tissue shows the most obvious fluctuation; the Cor curve of the liver metastasis from pancreatic cancer are the most flat; while those of the well and poor differentiated pancreatic cancer tissues fall in between.

In addition, the Cor curves as a function of θ for the normal pancreatic tissue show the sharpest peak [Fig. 6(b)], while the peaks of the Cor curves for the pancreatic tissues become less obvious from well differentiated pancreatic cancer tissue to the liver metastasis from pancreatic cancer. Therefore, the initial SHG images of the normal and the cancerous human pancreatic tissues can be distinguished by the patterns of the OD-GLCM Cor curves. Accordingly, the estimated value of orderliness decreases from the normal pancreatic tissue, to the well differentiated pancreatic cancer tissues, to the liver metastasis from pancreatic cancer (Table 3), which indicates that the structure of the collagen fibers gets more disordered as the pancreatic cancer progresses. The estimated fiber size may also be useful for the evaluation of pancreatic cancer, since it is possibly an indicator associated with the degradation and remodeling of collagen fibers during the pathological process. However, due to the limited sample size, the current data is insufficient to validate the value of the estimated fiber sizes in the discrimination of different pancreatic tissues (Table 3).

4 Discussion

4.1 Estimation of the Orderliness of Collagen Fibers in the Terms of the Scale

We have demonstrated that the orderliness of collagen fibers imaged by SHG microscope system can be assessed by the OD-GLCM Cor curves as a function of θ. Instead of the
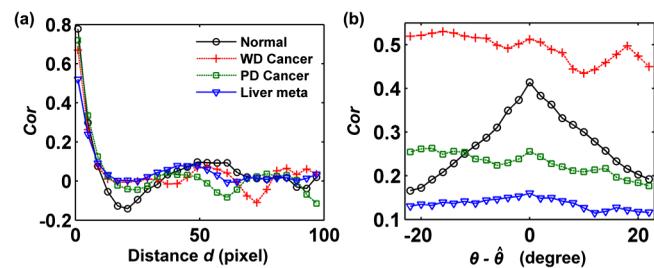
Fig. 6 The OD-GLCM Cor curves as a function of (a) d and (b) θ for the SHG images of normal and cancerous human pancreatic samples (Fig. 5). Normal, WD Cancer, PD Cancer, and Liver Meta represent the normal pancreatic tissue, the well differentiated pancreatic cancer tissue, the poor differentiated pancreatic cancer tissue, and the liver metastasis from pancreatic cancer, respectively. Note: OD-GLCM = orientation-dependent GLCM.

Table 3 The estimated orderliness and size of collagen fibers of the human pancreatic tissues.

	σ_{Cor}	Fiber size
Normal	0.07	8.2 μm (20 pixel)
WD Cancer	0.06	6.2 μm (15 pixel)
PD Cancer	0.03	10.3 μm (25 pixel)
Liver meta	0.01	7.0 μm (17 pixel)

evaluation from the aspect of the angle, the OD-GLCM Cor curves as a function of d calculated along the dominant orientation can also be used to describe the orderliness of collagen fibers in the terms of the scale.

For the model images and the SHG images of tendon samples, comparison analysis reveals that the d value corresponding to the inflexion of the OD-GLCM Cor curves calculated along the dominant orientation [Figs. 7(a) and 7(b)] gets lower as the collagen fibers become more disordered. For the discrimination of the pancreatic samples, the Cor curves show that the collagen fibers of the normal and well differentiated cancer tissues are

(a)

Legend: Model 1, Model 3, Model 2, Model 4

(b)

Legend: old, young

(c)

Legend: Normal, WD Cancer, PD Cancer, Liver meta

Fig. 7 The OD-GLCM Cor curves as a function of d calculated along the dominant orientation for (a) the model images, SHG images of (b) tendons and (c) pancreatic samples. Note: GLCM = gray level co-occurrence matrix; OD-GLCM = orientation-dependent GLCM.

more regular than those of the poor differentiated pancreatic cancer tissue and the liver metastasis from pancreatic cancer [Fig. 7(c)], which is consistent with the results mentioned above (Table 3).

4.2 Comparison Between the OD-GLCM Method and Other Commonly Used Methods for Texture Analysis

The other GLCM feature curves such as energy or angular second moment have been used to differentiate collagen fibers with different orderliness, such as aligned and randomly oriented fibers.[35] In our work, however, we found that the other GLCM features such as energy or angular second moment, contrast, and homogeneity (data not shown), resemble Cor that is dependent on the direction selected (Fig. 1). Therefore, it is more stable and accurate to use the OD-GLCM energy curves calculated based on the dominant orientation of the collagen fibers to reflect the orderliness of the texture. Moreover, the OD-GLCM method can provide quantitative indicators for the orderliness and the size of collagen fibers.

Other commonly used methods for the quantitative texture analysis include fast Fourier transforms (FFT) and the wavelet texture analysis (WTA) method.[20,21] The FFT method depends on a frequency decomposition of an image.[20] It has been used to evaluate the orientation index (or the anisotropy) of the SHG images of skin and corneal collagen fibers, which is effective for discrimination of collagen fibers with and without a particular orientation.[35,39,41] But the classification of different morphological patterns (linear, curved, or disordered) based on the estimation of the orderliness of collagen fibers has not been reported. Particularly, the estimation of the length of the sarcomeres, which have highly regular periodicity have been reported based on the FFT method.[42] However, it has not been assessed whether the FFT method is feasible for broad application in texture analysis of biomedical images, since large amounts of collagen fibers in the extracellular matrix of biological tissues are not as regular as the sarcomeres.

The WTA method is a space-frequency analysis of grey-level value variation based on wavelet transform,[20,21] and has been applied for the texture analysis of SHG images.[42] However, it is unable to provide the information directly associated with the morphology of collagen fibers such as the orderliness and the fiber size. Besides, WTA is generally considered to be a state-of-the-art method to reveal the directionality of different textures.[20,43] But it has never been validated for the application of texture analysis of the collagen fibers. Similar to the conventional GLCM method, the WTA method only uses features corresponding to the horizontal, vertical, and diagonal directions to analyze texture.[20] Since the orientation is an important texture characteristic of collagen fibers, this method may be more effective for biomedical applications when the dominant orientation of collagen fibers is taken into consideration.

Since GLCM is a kind of statistical approach for texture analysis, the accuracy of the estimated dominant orientation of collagen fibers depends on the number of the periodic units in the images. As can be observed for the model images, when there are more periodic units in the images, the estimated dominant orientation and fiber size are more close to the true value (Table 1). Therefore, the resulting estimation by OD-GLCM method depends on the size of the region of interest (ROI) after image rotation and cropping. Besides, for the completely random collagen fibers, the dominant orientation can hardly be
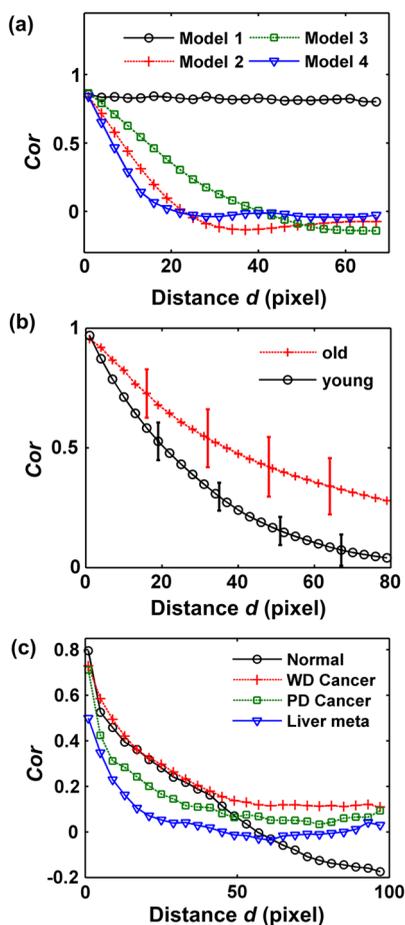
estimated, and the fiber size cannot be calculated accurately, either. Consequently, the OD-GLCM method is more effective for the description of the relatively ordered collagen fibers and the differentiation between the regular and random collagen fibers.

Comparatively speaking, based on the estimation of the dominant orientation of collagen fibers, the OD-GLCM method can not only distinguish different texture patterns, but also provide more comprehensive information quantitatively related with the orderliness and size of collagen fibers for the relatively ordered collagen fibers.

4.3 Further Application to Clinical Evaluation

In this paper, the number of human pancreatic samples is rather small and the quantitative analysis is statistically limited. There is still some distance to go before the OD-GLCM can be used to diagnose and stage pancreatic cancer. For the clinical evaluation of different types of tissues, a larger number of human pancreatic samples should be examined to eliminate individual differences in a further study, so that the morphological alterations of collagen fibers between normal and cancerous human pancreatic tissues at different stages can be statistically characterized. Careful investigations on the selection of the fields of view and the interpretation of the quantitative parameters are required, and other quantitative methods (such as the evaluation of the content of collagen fibers) can also be complemented to provide comprehensive information associated with the progression of pancreatic cancer. Meanwhile, the corresponding histological outcomes need to be represented to validate the results of the SHG imaging.

5 Conclusion

We have developed the OD-GLCM method for the quantitative texture analysis, since the dominant orientation of the collagen fibers is usually ignored in the conventional GLCM analysis, which is an important characteristic of collagen fibers with a filamentous structure. The calculation of the OD-GLCM feature curves was based on the estimated dominant orientation of collagen fibers. We demonstrated that the OD-GLCM method is more effective than conventional GLCM method in discriminating collagen fibers of tendons from rats with different ages. Moreover, additional information including the orderliness and the size of the collagen fibers can be obtained using the OD-GLCM method. The OD-GLCM method was applied to discriminate the preliminary SHG images of different types of human pancreatic tissues. The method has potential applications in the diagnosis and staging of diseases marked with abnormal collagen morphology.

References

1. W. Friess, "Collagen—biomaterial for drug delivery," *Eur. J. Pharm. Biopharm.* **45**(2), 113–136 (1998).
2. T. Hompland et al., "Second-harmonic generation in collagen as a potential cancer diagnostic parameter," *J. Biomed. Opt.* **13**(5), 054050(2008).
3. C. Bayan et al., "Fully automated, quantitative, noninvasive assessment of collagen fiber content and organization in thick collagen gels," *J. Appl. Phys.* **105**(10), 102042 (2009).
4. N. D. Kirkpatrick, M. A. Brewer, and U. Utzinger, "Endogenous optical biomarkers of ovarian cancer evaluated with multiphoton microscopy," *Cancer Epidemiol. Biomarkers Prev.* **16**(10), 2048–2057 (2007).
5. G. Chen et al., "Nonlinear spectral imaging of human hypertrophic scar based on two-photon excited fluorescence and second-harmonic generation," *Br. J. Dermatol.* **161**(1), 48–55 (2009).
6. C. M. Hsueh et al., "Multiphoton microscopy: a new approach, in physiological studies and pathological diagnosis for ophthalmology," *J. Innovative Opt. Health Sci.* **2**(1), 45–60 (2009).
7. K. Lu et al., "Non-linear spectral imaging microscopy studies of human hypertrophic scar," *J. Innovative Opt. Health Sci.* **2**(1), 61–66 (2009).
8. P. Wilder-Smith et al., "In vivo multiphoton fluorescence imaging: a novel approach to oral malignancy," *Lasers Surg. Med.* **35**(2), 96–103 (2004).
9. O. Nadiarnykh et al., "Second harmonic generation imaging microscopy studies of osteogenesis imperfecta," *J. Biomed. Opt.* **12**(5), 051805 (2007).
10. A. Zoumi, A. Yeh, and B. J. Tromberg, "Imaging cells and extracellular matrix in vivo by using second-harmonic generation and two-photon excited fluorescence," *Proc. Natl. Acad. Sci. USA* **99**(17), 11014–11019 (2002).
11. E. Georgiou et al., "Second and third optical harmonic generation in type I collagen, by nanosecond laser irradiation, over a broad spectral region," *Opt. Commun.* **176**(1–3), 253–260 (2000).
12. S. V. Plotnikov et al., "Characterization of the myosin-based source for second-harmonic generation from muscle sarcomeres," *Biophys. J.* **90**(2), 693–703 (2006).
13. L. K. Soh and C. Tsatsoulis, "Texture analysis of SAR sea ice imagery using gray level co-occurrence matrices," *IEEE Trans. Geosci. Rem. Sens.* **37**(2), 780–795 (1999).
14. R. M. Williams, W. R. Zipfel, and W. W. Webb, "Interpreting second-harmonic generation images of collagen I fibrils," *Biophys. J.* **88**(2), 1377–1386 (2005).
15. P. Friedl, "Dynamic imaging of cellular interactions with extracellular matrix," *Histochem. Cell Biol.* **122**(3), 183–190 (2004).
16. E. Brown et al., "Dynamic imaging of collagen and its modulation in tumors in vivo using second-harmonic generation," *Nat. Med.* **9**(6), 796–800 (2003).
17. P. J. Campagnola and L. M. Loew, "Second-harmonic imaging microscopy for visualizing biomolecular arrays in cells, tissues and organisms," *Nat. Biotechnol.* **21**(11), 1356–1360 (2003).
18. G. Cox et al., "3-dimensional imaging of collagen using second harmonic generation," *J. Struct. Biol.* **141**(1), 53–62 (2003).
19. W. R. Zipfel et al., "Live tissue intrinsic emission microscopy using multiphoton-excited native fluorescence and second harmonic generation," *Proc. Natl. Acad. Sci. USA* **100**(12), 7075–7080 (2003).
20. M. H. Bharati, J. J. Liu, and J. F. MacGregor, "Image texture analysis: methods and comparisons," *Chemom. Intell. Lab. Syst.* **72**(1), 57–71 (2004).
21. G. Castellano et al., "Texture analysis of medical images," *Clin. Radiol.* **59**(12), 1061–1069 (2004).
22. A. Al-Janobi, "Performance evaluation of cross-diagonal texture matrix method of texture analysis," *Pattern Recogn.* **34**(1), 171–180 (2001).
23. D. A. Clausi and M. E. Jernigan, "A fast method to determine co-occurrence texture features," *IEEE Trans. Geosci. Rem. Sens.* **36**(1), 298–300 (1998).
24. B. Tian et al., "A study of cloud classification with neural networks using spectral and textural features," *IEEE Trans. Neural. Network* **10**(1), 138–151 (1999).
25. F. Kayitakire, C. Hamel, and P. Defourny, "Retrieving forest structure variables based on image texture analysis and IKONOS-2 imagery," *Rem. Sens. Environ.* **102**(3–4), 390–401 (2006).

26. E. S. Gadelmawla, "A vision system for surface roughness characterization using the gray level co-occurrence matrix," *NDT & E International* **37**(7), 577–588 (2004).

27. G. Bartolacci et al., "Application of numerical image analysis to process diagnosis and physical parameter measurement in mineral processes — Part I: flotation control based on froth textural characteristics," *Miner. Eng.* **19**(6–8), 734–747 (2006).

28. A. V. Alvarenga et al., "Complexity curve and grey level co-occurrence matrix in the texture evaluation of breast tumor on ultrasound images," *Med. Phys.* **34**(2), 379–387 (2007).

29. G. A. Losa and C. Castelli, "Nuclear patterns of human breast cancer cells during apoptosis: characterisation by fractal dimension and co-occurrence matrix statistics," *Cell Tissue Res.* **322**(2), 257–267 (2005).

30. F. Chabat, G. Z. Yang, and D. M. Hansell, "Obstructive lung diseases: texture classification for differentiation at CT," *Radiol.* **228**(3), 871–877 (2003).

31. W. Chen et al., "Volumetric texture analysis of breast lesions on contrast-enhanced magnetic resonance images," *Magn. Reson. Med.* **58**(3), 562–571 (2007).

32. D. M. U. Sabino et al., "A texture approach to leukocyte recognition," *R. Time. Imag.* **10**(4), 205–216 (2004).

33. J. E. Wilhjelm et al., "Quantitative analysis of ultrasound B-mode images of carotid atherosclerotic plaque: correlation with visual classification and histological examination," *IEEE Trans. Med. Imag.* **17**(6), 910–922 (1998).

34. D. Mahmoud-Ghoneim et al., "Three dimensional texture analysis in MRI: a preliminary evaluation in gliomas," *Magn. Reson. Imag.* **21**(9), 983–987 (2003).

35. R. Cicchi et al., "Scoring of collagen organization in healthy and diseased human dermis by multiphoton microscopy," *J. Biophotonics* **3**(1–2), 34–43 (2010).

36. R. M. Haralick, K. Shanmugam, and I. H. Dinstein, "Textural Features for image classification," *IEEE Trans. Syst. Man Cybern.* **3**(6), 610–621 (1973).

37. A. Zoumi et al., "Imaging coronary artery microstructure using second-harmonic and two-photon fluorescence microscopy," *Biophys. J.* **87**(4), 2778–2786 (2004).

38. T. T. Le et al., "Label-free molecular imaging of atherosclerotic lesions using multimodal nonlinear optical microscopy," *J. Biomed. Opt.* **12**(5), 054007 (2007).

39. P. Matteini et al., "Photothermally-induced disordered patterns of corneal collagen revealed by SHG imaging," *Opt. Express* **17**(6), 4868–4878 (2009).

40. A. Baraldi and F. Parmiggiani, "An investigation of the textural characteristics associated with gray level co-occurrence matrix statistical parameters," *IEEE Trans. Geosci. Rem. Sens.* **33**(2), 293–304 (1995).

41. S. L. Wu et al., "Quantitative analysis on collagen morphology in aging skin based on multiphoton microscopy," *J. Biomed. Opt.* **16**(4), 040502 (2011).

42. S. Plotnikov et al., "Optical clearing for improved contrast in second harmonic generation Imaging of skeletal muscle," *Biophys. J.* **90**(1), 328–339 (2006).

43. A. Lefebvre, T. Corpetti, and L. H. Moy, "Estimation of the orientation of textured patterns via wavelet analysis," *Pattern Recogn. Lett.* **32**(2), 190–196 (2011).